Nat Hazards (2015) 79:317–330
DOI 10.1007/s11069-015-1844-1

ORIGINAL PAPER

Identifications and removal of diurnal and semidiurnal variations in radon time series data of Hsinhua monitoring station in SW Taiwan using singular spectrum analysis

Arvind Kumar[1] · Vivek Walia[1] · Baldev Raj Arora[1,4] · Tsanyao Frank Yang[2] · Shih-Jung Lin[1] · Ching-Chou Fu[2] · Cheng-Hong Chen[2] · Kuo-Liang Wen[1,3]

Received: 24 December 2014 / Accepted: 30 May 2015 / Published online: 11 June 2015

Abstract Over the past three decades, anomalous temporal changes in radon concentrations have been reported in relation to earthquake occurrences. However, radon anomalies in all cases are not only controlled by seismic activity, but also by meteorological parameters which make isolation of earthquake precursory signals complicated. In the present study, characteristics of temporal variability of soil gas radon concentrations at the Hsinhua monitoring station, southern Taiwan, have been examined using singular spectrum analysis (SSA). In order to make continuity and regularity of the data before applying the SSA, the radon data were carefully edited for gaps and discontinuous jumps following intervals of malfunctioning of equipments. Digital filter has been applied in eliminating the long-term trend in the data and retains variations of <30 days. The radon changes exhibit dominant daily variations, which are controlled by atmospheric temperature inducted evaporation in surface water saturated soil (capping effect). The causal relationship is marked by a clear phase lag of 2–3 h in the sense that peak in the daily variation of radon succeeds the peak in temperature. Aperiodic variations in soil radon intensity in the range of 2–10 days are negatively correlated with temperature, while positively correlated with pressure. However, the negative correlation of the soil radon with temperature is found to be pseudo-effect arising due to interrelation between temperature and pressure.

✉ Vivek Walia
vivekwalia@rediffmail.com; walia@ncree.org.tw

Arvind Kumar
kumararvind79@hotmail.com; kumar@ncree.narl.org.tw

[1] National Center for Research on Earthquake Engineering, National Applied Research Laboratories, Taipei 106, Taiwan

[2] Department of Geosciences, National Taiwan University, Taipei 106, Taiwan

[3] Department of Earth Sciences and Institute of Geophysics, National Central University, Jhongli 32001, Taiwan

[4] Division of Seismology, Ministry of Earth Sciences, New Delhi 110003, India

Keywords Radon time series · Singular spectrum analysis · Meteorological parameters · Hsinhua monitoring station · Taiwan

1 Introduction

Earthquakes are the worst natural calamities which occur in some parts of the world with little or no warning. These earthquakes not only cause immediate loss of life and property, but also make a long-term adverse impact on the overall economy of the country. Taiwan is one of the most active seismic regions of the world with an average of about 20,000 earthquakes occurring every year in or around it as reported by the Central Weather Bureau of Taiwan (2011–2012) (www.cwb.gov.tw). Despite several years of research, the use of advanced equipment and the efforts of many dedicated scientists, the task of predicting earthquakes is still a distant goal. Since the 1960s, geochemical signals preceding significant earthquakes have been used for earthquake prediction study worldwide (Yang et al. 2005, 2011; Hartmann and Levy 2005; Italiano et al. 2008; Einarsson et al. 2008; Cicerone et al. 2009; Kumar et al. 2009, 2013a, b; Walia et al. 2009, 2013). Among the potential geochemical precursors, radon changes are probably the most frequently used for earthquake monitoring/predicting purposes. The first evidence of a correlation between radon and earthquake occurrence came from observations of radon concentration in well water, prior to the Tashkent earthquake of 1966 (Ulomov and Mavashev 1967). Radon (^{222}Rn) is a daughter nuclide of radium (^{226}Ra), which in turn comes from the long-lived antecedent, uranium (^{238}U). The short half-life of ^{222}Rn (3.82 days) limits its diffusion in soil, so the radon measured at the ground surface cannot be released from a deeper origin, unless there exists a driving mechanism other than mere diffusion. However, radon anomalies are not only controlled by seismic activity, but also by meteorological parameters such as soil moisture, rainfall, temperature and barometric pressure (Ghosh et al. 2009; Stranden et al. 1984; Walia et al. 2005). This makes it complicated and, for small earthquakes, often impossible to differentiate between those anomalies caused by seismic events and those caused solely by atmospheric changes. Therefore, the application of theoretical and empirical algorithms for removing meteorological effects is necessary (Choubey et al. 2009; Ramola et al. 2008; Torkar et al. 2010; Zmazek et al. 2003). Various mathematical modelings were also proposed by some workers. However, as per our present understanding, it is very difficult to explore the complex phenomena of seismic-induced radon emanation process by means of conventional mathematical modeling and statistical analysis. Nonlinear methods such as power spectrum analysis, wavelet analysis, and fractal analysis may assist to reveal nonlinear characteristics of the underearth physicochemical mechanism involved in the radon emanation process. In the present study, characteristics of temporal variability of soil gas radon concentrations at the established earthquake monitoring station along the Hsinhua Fault in Tainan area, southern Taiwan, have been examined using singular spectrum analysis (SSA) with the aim of the appraisal and filtrations of environmental/meteorological parameters on radon emission. In recent years, SSA, a relatively novel but powerful technique in time series analysis, has been developed and applied to many practical problems across different fields [e.g., Fraedrich (1986), Vautard and Ghil (1989)]. The main idea of SSA is to apply the principal component analysis to the trajectory matrix obtained from the original time series with subsequent reconstruction of the series.

The Hsinhua Fault is recognized as one of the active faults in southwestern Taiwan (Fig. 1a). It was considered to be right-lateral strike-slip fault, and the last movement on it occurred in 1946 accompanied by an earthquake ($M = 6.3$) (Hsu and Chang 1979; Chang et al. 1947). But later studies of Lee et al. (2000) using seismic data identified it as a back-thrust fault dipping north 17° at great depth and at a high angle of 70° near the surface. It is located in the coastal plain and foothills in the southwestern part of Taiwan, about 10 km northeast of Tainan City. Some studies have shown that this fault is not only the 1946 earthquake fault, but also a fault that has moved many times in the past (Hsu and Chang 1979; Hwang et al. 2003). The total length of the fault in the subsurface probably was 12 km or more (Fig. 1b). Judging from its location, orientation and sense of slip, this structure is also likely to be an accommodation structure in the transition zone (Lee et al. 2000). The presence of some major tectonic elements including Chukou Fault, Tsochen Fault, Napalin Anticline, Shihtzuchi Syncline in the foothills belt and Kuanmiao Syncline in the Tainan basin around the studied Hsinhua fault is the part of fold and thrust belt that formed during the Penglai Orogeny. The major formation in the area is Liushuang Formation besides terrace and alluvium. Upper part of Liushuang Formation is predominantly composed of brown-yellowish sandstone, while the lower part is thick mudstone. Terrace and alluvium comprise mainly uncemented sand, mud, gravels and pebbles.

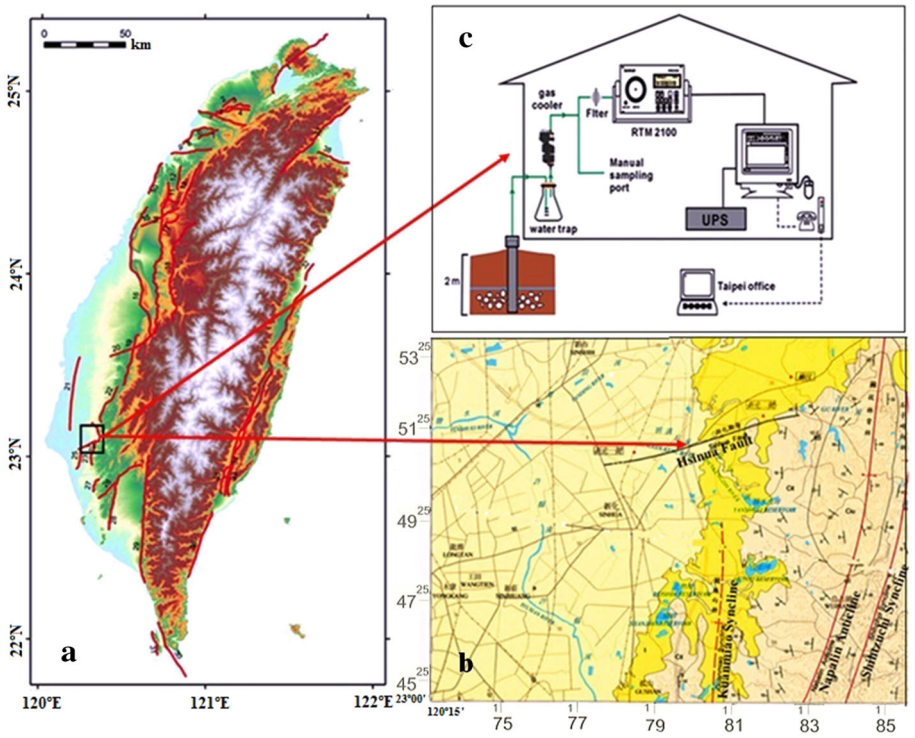

Fig. 1 **a** *Map* showing the active faults (*red lines*) in Taiwan and the location of radon monitoring station. **b** *Enlarge view* of Hsinhau Fault. **c** *Sketch* showing the scheme at the monitoring station

2 Radon monitoring station setup

Before selection of a monitoring site at Hsinhua Fault, the occurrence of deeper gas emanation was investigated by the soil gas surveys and followed by continuous monitoring of some selected sites with respect to tectonic activity to check the sensitivity of the sites (Walia et al. 2009). To build a monitoring station, reconstructions of all the selected points have been done by digging holes of 2 m and by casing these holes with PVC pipes. At the bottom of PVC pipe, a fine mesh is attached to avoid any unwanted materials to enter the pipe. The PVC sheet is put on all the sides of the PVC pipe at the bottom covering about 1 m on all sides; this avoids the rainwater to enter into the hole. Some pebbles were also put at the bottom to reduce the meteorological effects before filling the sides of the holes. A site has been selected for long-term monitoring on the basis of coexistence of high concentration of helium, radon and carrier gases and sensitivity toward the tectonic activity in the region. After the site selection, a continuous monitoring station has been established using radon detectors RTM 2100 along with the carbon dioxide detector. After passing through the water trap and gas cooler, the soil gas is transferred into an alpha spectroscopy (SARAD-RTM2100) via an internal pump for radon and thoron measurement (Fig. 1c) with a sampling interval of 15 min. All the data have been transferred to the office via the Internet for further analysis. Data of rainfall and seismic parameters (viz. earthquake parameters, intensity at a monitoring station, etc.) were obtained from Central Weather Bureau of Taiwan (2011–2012) (www.cwb.gov.tw).

3 Analysis of radon time series data

In the present study, characteristics of temporal variability of soil gas radon concentrations at the Hsinhua monitoring station, southern Taiwan, have been examined using SSA (Vautard et al. 1992). In order to make continuity and regularity of the data before applying the SSA, the radon data were carefully edited for gaps and discontinuous jump following intervals of malfunctioning of equipments. Digital filter has been applied in eliminating the long-term trend in the data and retains variations of <30 days. SSA exploits the lag-correlation structure of the time series to extract aperiodic trends and quasi-periodic component of the original time series. If $\rho_0, \rho_1, \rho_2, \ldots, \rho_{M-1}$ are the first M auto-correlations of the time series, then the lag correlation with the Toeplitz structure is generated as

$$\frac{1}{M}\begin{vmatrix} \rho_0 & \rho_1 & \rho_2 & \cdots & \rho_{M-1} \\ \rho_1 & \rho_0 & \cdots & & \rho_0 \\ \cdots & \cdots & \cdots & & \\ \rho_{M-1} & \rho_{M-2} & \cdots & & \rho_0 \end{vmatrix}$$

which is then subjected to eigenanalysis to get the eigenvalues in descending order and the corresponding eigenvectors.

In SSA, small number of eigenvalues can collectively reproduce the salient feature of the time series. The greatest advantage of SSA, in contrast to power spectral analysis, is its ability to generate individual time series of the reconstructed components whose evolution with time can be graphically seen for interpretation of these oscillations, their intermittancy and identification of possible causative mechanisms.

Furthermore, the relative contribution of the individual components to the total variance of the time series is obtained so that we can identify and isolate significant trends and quasi-periodic fluctuations of the noisy part of the data.

4 Results and discussion

The continuity and regularity of the data are prerequisites before using any application of statistical and numerical tools to identify influences of meteorological parameters on radon emission. After careful examining of the Hsinhua station radon data, we have selected data for interval with minimum breaks and jumps (Fig. 2). The 15-min data were carefully edited for gaps and discontinuous jump following intervals of malfunctioning of equipments. The allied meteorological parameters, viz. atmospheric pressure, temperature, humidity, precipitation (rainfall) data from Central Weather Bureau of Taiwan nearest station were obtained. Since allied meteorological data were available with hourly sampling, 15-min radon were also reduced to hourly averages. Also, all the data were normalized around the threshold values, i.e., mean values. Since primary objective was to search for short-term earthquake precursory signals, which on global experience show characteristic changes on a timescale of 2–3 weeks, the selected time series of hourly values were subjected to high-pass digital filtration. Butterworth filter cleaned the data for any variations with period more than 30 days. Figure 2 shows the observed (blue curve) and filtered (red curve) radon time series at the Hsinhua monitoring station from November 12, 2011, to February 28, 2012. Continuous soil gas radon monitoring has been started in Taiwan since January 2006, so in the present study, day number starts from that date. The

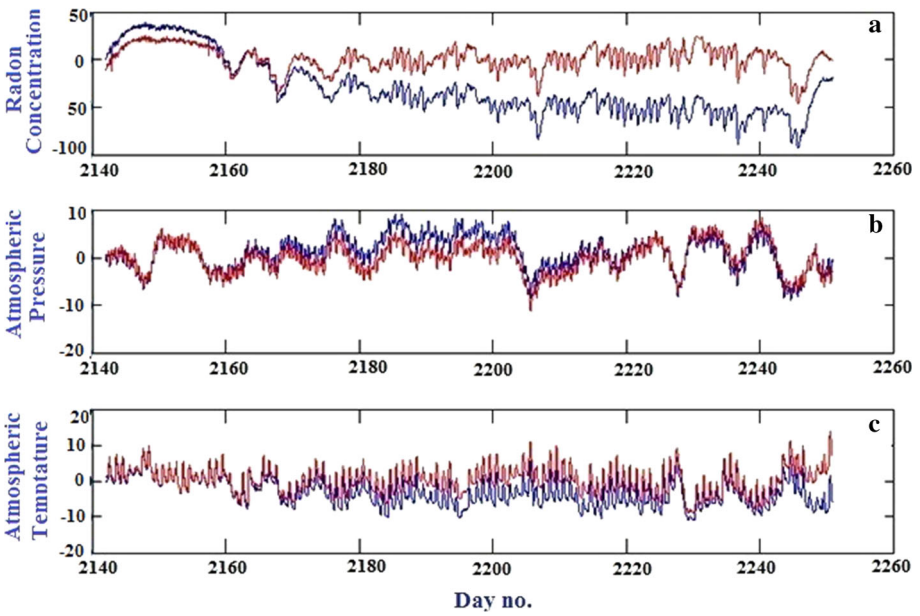

Fig. 2 Observed and filter time series of **a** radon, **b** atmospheric pressure, **c** atmospheric temperature, at Hsinhau from November 12, 2011 to February 28, 2012

observed radon time series data of Hsinhua monitoring station show the variation from about +50 to −100 after the normalization. Such variation in radon time series data has been removed using the Butterworth filter (red curve). Butterworth filter is also used in atmospheric temperature and atmospheric pressure time series data for the selected period. But there were not much variations in the atmospheric temperature and atmospheric pressure time series data, so observed (blue curve) and filtered (red curve) time series data of atmospheric temperature and atmospheric pressure are almost same (Fig. 2).

SSA analysis is intricately knit around fast Fourier transformation, and this requirement required that length of time series is having some power of 2. To meet this requirement, time section corresponding to a length of 2048 h starting with effect from November 29, 2011, was used. Auto-correlations up to lag of 300 were calculated. Choice of relatively low value ensured stability of resolving waveforms. Figure 3 shows the decomposed first 6 eigenvalues (EV) for radon time series using SSA. The singular value decomposition (SVD) to radon data showed that first 6 eigenvalues accounted for 96 % of the variance of the individual time series (Fig. 3). As noted, eigenvalue represented by EV-1, EV-3 and EV-4 dominantly represented aperiodic components, whereas EV-2 and EV-5 represented periodic components corresponding to diurnal and semidiurnal variation. Radon variations have dominant daily variations, accounting to 19 % of the total variance in radon at the Hsinhua monitoring station. These decomposed eigenvectors in radon grouped into two classes as aperiodic components and periodic components (diurnal and semidiurnal variation). The sum of EV-1, EV-3 and EV-4 in the first group account for 68 % variation and

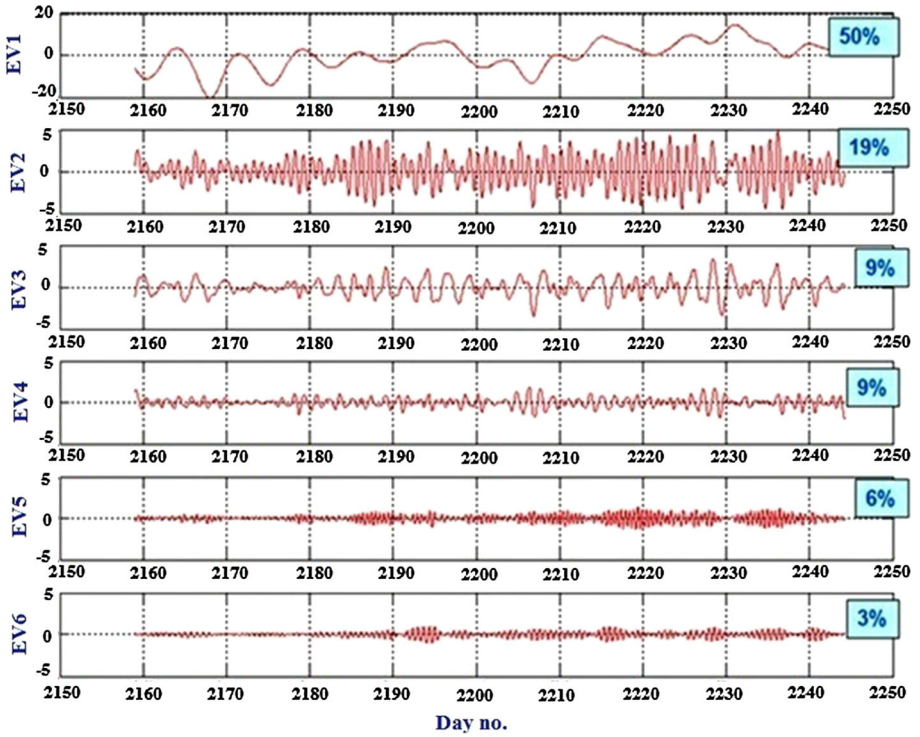

Fig. 3 Plot of decomposed eigenvector in radon at Hsinhau from November 29, 2011 to February 22, 2012

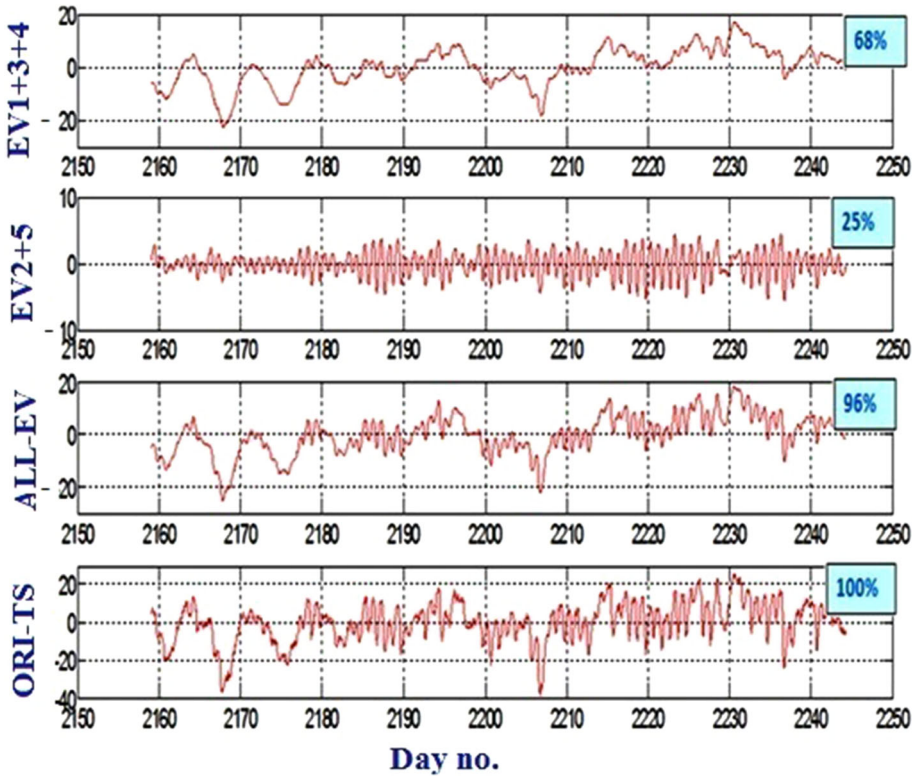

Fig. 4 Plot of decomposed eigenvector in radon grouped into two classes at Hsinhau from November 29, 2011 to February 22, 2012

in second group EV-2 and EV-5 together account for 25 % of the variation (Fig. 4). Figures 5 and 6 show the decomposed first eigenvalues (EV) for atmospheric temperature and atmospheric pressure time series using SSA. The first 4 eigenvalues from singular value decomposition (SVD) to atmospheric temperature and atmospheric pressure data accounted nearly for 93 and 96 %, respectively, of the variation of the individual time series. This means singular value decomposition (SVD) to radon, and temperature/pressure data showed that the first 4 or 5 eigenvalues (EV) accounted for nearly 95 % of the variance of the individual time series, which is the interesting aspect that sum of just first 4 or 5 EVs is able to reproduce the most salient features of the total variation, and more significantly synthesized variations are largely free from the background natural variations.

Atmospheric pressure variations have dominant semidiurnal variations, accounting to 18 % of the total variation in atmospheric pressure at the Hsinhua monitoring station. But atmospheric temperature variations have dominant daily variations like radon variation, accounting to 18 % of the total variance in atmospheric temperature at the Hsinhua monitoring station. This means that daily variations of radon emission at Hsinhua are controlled by atmospheric temperature. Figures 7 and 8 show decomposed eigenvector in atmospheric temperature as well as in atmospheric pressure grouped into two classes as aperiodic components and periodic components. It is the common feature of various time

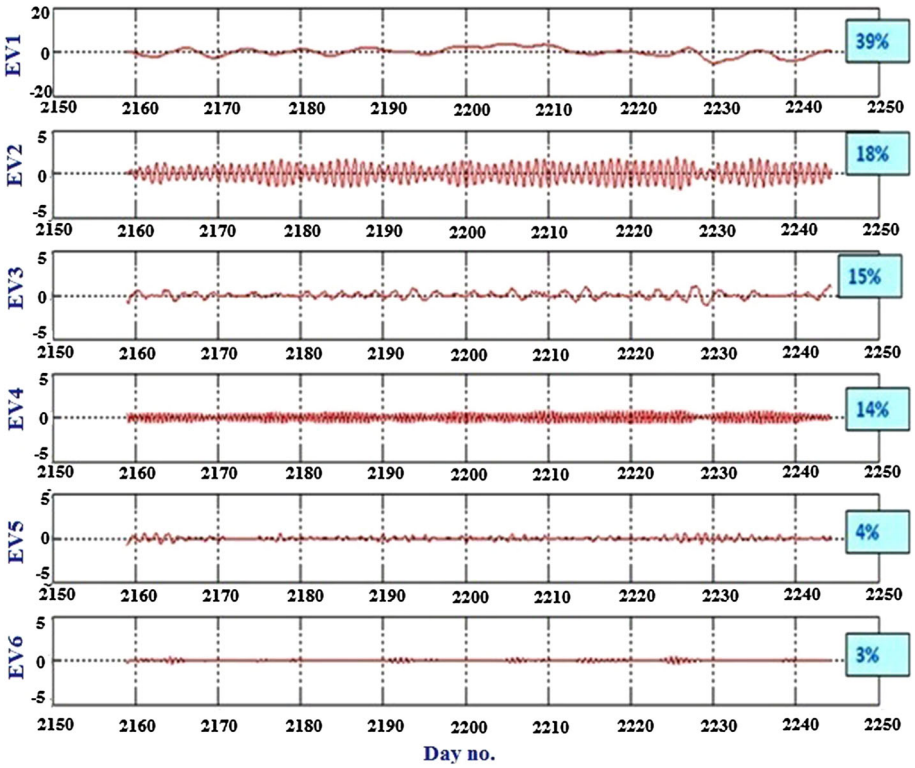

Fig. 5 Plot of decomposed eigenvector in atmospheric temperature at Hsinhau from November 29, 2011 to February 22

series that in their SVD, the waveforms of major constituting EV can be grouped into two classes.

In order to study the effect of temperature and pressure in the variation of radon emission at the Hsinhua monitoring station, the correlation and partial correlation between periodic/aperiodic components of radon with temperature and pressure have been calculated. Figure 9 shows the correlation and partial correlation between aperiodic components of radon with temperature and pressure, whereas Fig. 10 shows the correlation and partial correlation between periodic components of radon with temperature and pressure. It is clear from the Fig. 9 for aperiodic variation, that radon is negatively correlated with temperature, but it is found to be pseudo-effect arising due to parallel variation in pressure. For periodic variation, daily variations of radon emission at Hsinhua are controlled by atmospheric temperature affecting evaporation in surface water saturated soil (capping effect). Radon is negatively correlated with temperature, whereas positively correlated with pressure (Fig. 10).

The decomposed EVs corresponding to periodic as well as aperiodic components show dependence on atmospheric temperature as pressure. The exact nature and degree of dependence of the radon on temperature and pressure is examined by correlation analysis. It becomes clear that aperiodic components of radon is negatively correlated with temperature (−0.4) but positively correlated with pressure (0.4). Both these correlation

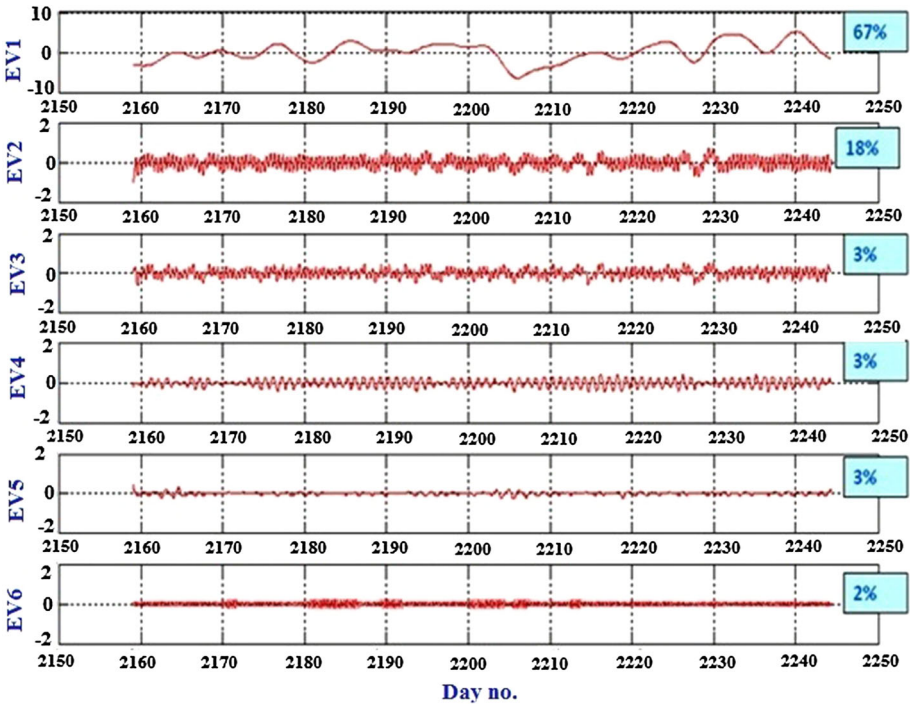

Fig. 6 Plot of decomposed eigenvector in atmospheric pressure at Hsinhau from November 29, 2011 to February 22

coefficient using 2048 pair of data points are significant at 95 % confidence level. However one also observes that temperature and pressure themselves are anti-correlated (−0.55). Hence it becomes difficult to arrive at the conclusion whether radon variability is controlled by temperature or pressure variation. To resolve this, we take re-course to partial correlation where the correlation of one parameter with other is examined statistically, keeping the effect of variability of third parameter constant. The partial correlation coefficient between periodic component of radon with temperature, with the influence of atmospheric pressure eliminated, is much reduced (i.e. −0.1) and statistically not significant. It emerges that dependence of radon on temperature is apparently due to the pseudo effect arising due to the interrelation between temperature and pressure. In contrast, the influence of pressure on radon variability persists even when effect of temperature variability is removed (0.5). It is found that ∼25 % of the percentage variability (square of partial correlation multiplied with 100) arises from the variation in pressure and the contribution of atmospheric temperature is negligible, only about 1 %. Similar statistics in respect of periodic component is rather physically less viable as periodic variations in radon is admixture of diurnal and semi-diurnal variations, where corresponding variations in atmospheric temperature is dominantly diurnal where pressure variations are primarily semidiurnal. The diurnal periodic component in radon again shows strong negative dependence but the peak correlation is observed with a time lag of 2–3 hours. The peak correlation of diurnal radon and temperature at time lag of 3 hours is −0.5 and this does not change even when effect of pressure variations are removed by partial correlation. The

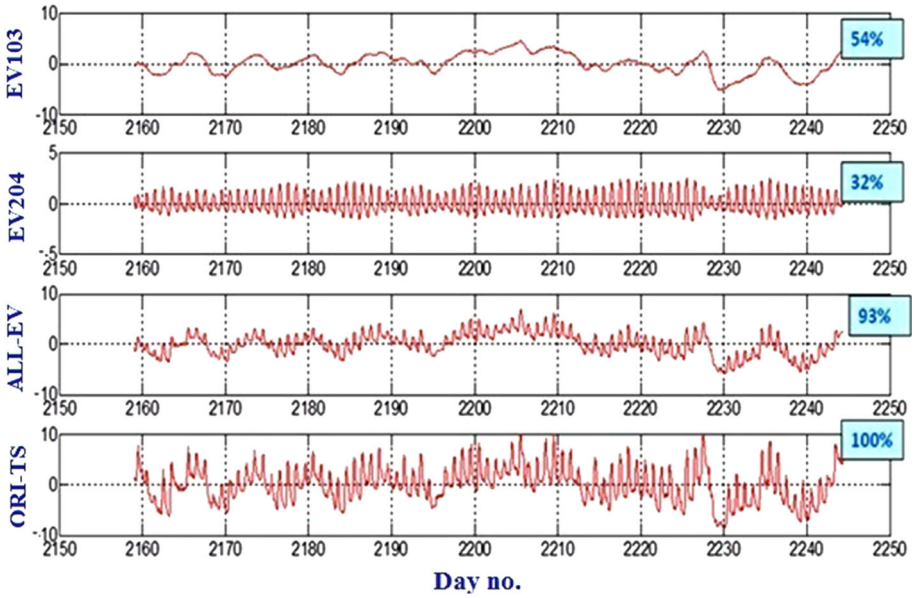

Fig. 7 Plot of decomposed eigenvector in atmospheric temperature grouped into two classes at Hsinhau from November 29, 2011 to February 22, 2012

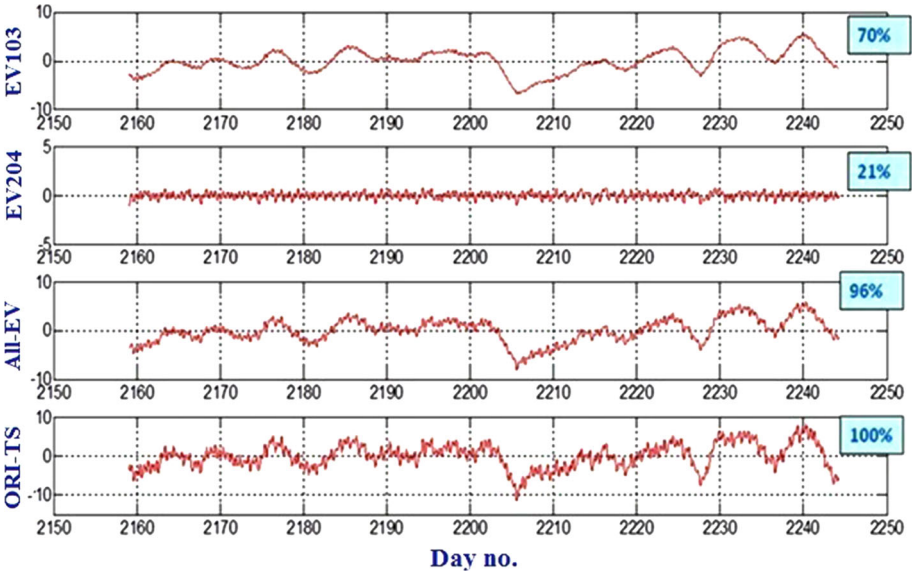

Fig. 8 Plot of decomposed eigenvector in atmospheric pressure grouped into two classes at Hsinhau from November 29, 2011 to February 22, 2012

semi-diurnal variations in radon show nearly similar dependence on pressure with correlation coefficient of 0.33. In sum up, periodic component in radon again shows nearly 25 percent of variability due to diurnal component of temperature and $\sim$10 percent of

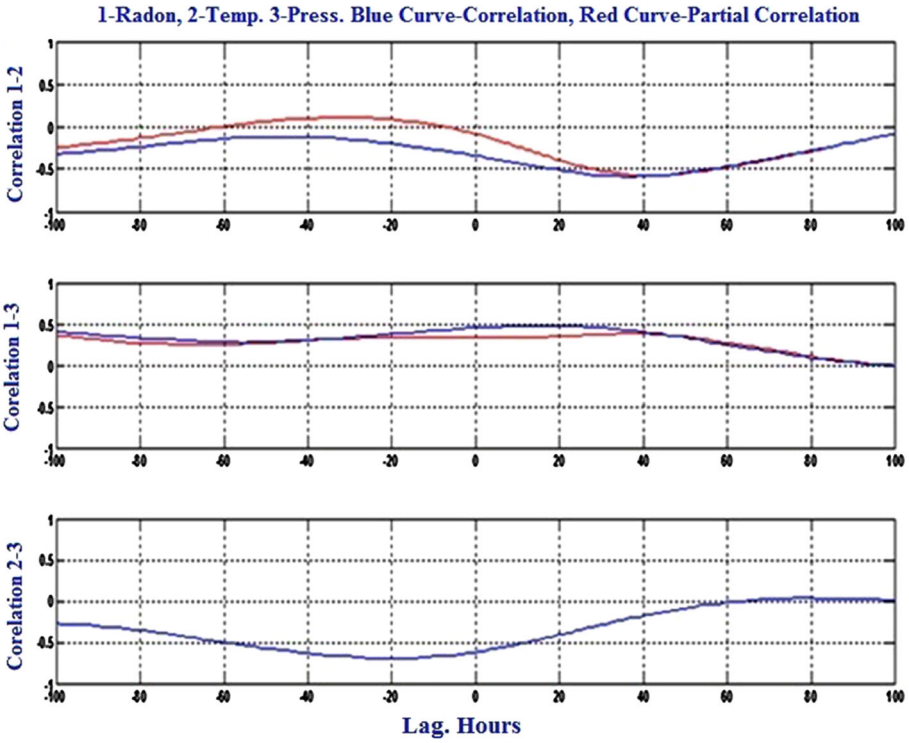

Fig. 9 Correlations of aperiodic component of radon with temperature and pressure at Hsinhau

variability due to semi-diurnal pressure variations. In this periodic component time lag of 2–3 hours implies that peak in radon occurs 2–3 hour succeeds peak value of the controlling meteorological factors. The influence of temperature on radon variability at diurnal period may be controlled by the temperature dependent evaporation of moisture from the top soil cover (capping effect), which control the escape of radon from top soil layer to space and visa-a-versa. The influence of pressure may be determined by the well-known processed of diffusion.

An obvious advantage of the application of the SSA technique is that we have better understanding of the nature and extent of the control of meterorological parameters, viz. temperature and pressure, on the radon variability. The radon variations cleaned up for these parameters can be more efficiently used to study the effects of individual rainfall sequences as well as search effect of earthquake occurrence on radon. Radon time series after cleaning for diurnal and semidiurnal variation is presented in Fig. 11 along with the earthquakes and rainfall events occurred in the same period. Rainfall recorded is very small (<2 mm), and a total of seven local earthquake events (epicentral's distance <50 km) with magnitude ranging from 3.1 to 4.8 M, which fit criteria to produce precursors established earlier by Walia et al. (2013). It is clear from the figure that most of the time radon starts to decrease following the rainfall or has no effects on radon emission (Fig. 11). However, there is also suggestions radon values are positive and/or increase before the occurrence of earthquake. The separation and quantification of rainfall influence and charcaterisation of earthquake precursory signals is a subject of future paper in progress.

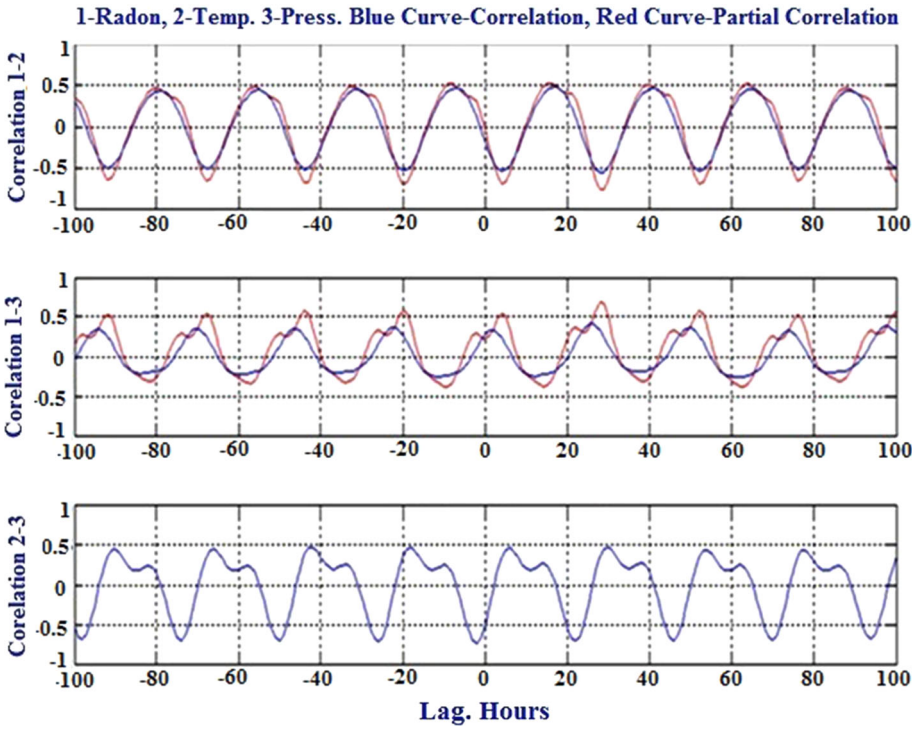

Fig. 10 Correlations of aperiodic component of radon with temperature and pressure at Hsinhau

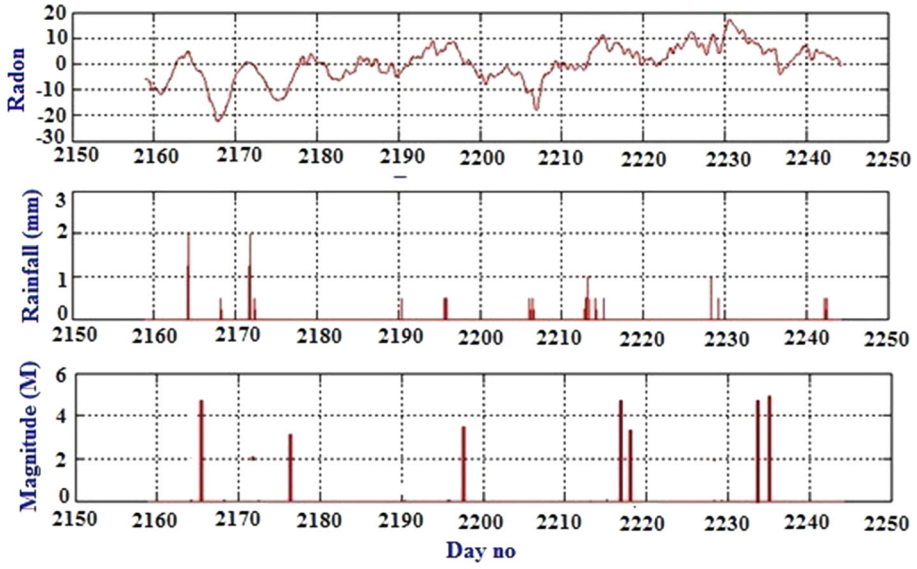

Fig. 11 Plot of radon, rainfall and earthquake at Hsinhau from November 29, 2011 to February 22, 2012

5 Conclusions

From this study, we can conclude that:

- Digital filter helps in eliminating the long-term trend in the data and retains variations of less than 30 days.
- An SSA method removes diurnal and semidiurnal oscillations from soil radon data time series in order to better relate seismic activities to changes in soil radon concentration.
- Radon has dominant daily variations. The later is accounting for 19 % of the total variance in radon at the Hsinhua monitoring station.
- Daily variations of radon emission at Hsinhua are controlled by atmospheric temperature affecting evaporation in surface water saturated soil (capping effect).
- For periodic variation, radon is negatively correlated with temperature, whereas positively correlated with pressure.
- For aperiodic variation, radon is negatively correlated with temperature, but it is found to be a pseudo-effect arising due to parallel variation in pressure.

Acknowledgments This manuscript is dedicated to the co-author Prof. Tsanyao Frank Yang (TFY), who passed away on 12th March 2015. Born in 1961, TFY worked for many years at the Department of Geosciences, National Taiwan University (NTU), Taipei in Taiwan. He was a tireless worker, contributing greatly, both organizationally and scientifically. He is greatly missed within the Earth science community and beyond, especially by those of us who worked closely with him and also knew him as a good friend. The authors are grateful for the anonymous reviewer's valuable comments that improved the manuscript. The authors are also thankful to the Ministry of Science and Technology (MOST) of Taiwan for partially supporting this work financially under the projects (MOST 103-2116-M-492 -002 & MOST 103-2811-M-492-004). The authors are grateful for the anonymous reviewer's valuable comments that improved the manuscript. The authors are also thankful to the Ministry of Science and Technology (MOST) of Taiwan for partially supporting this work financially under the projects (MOST 103-2116-M-492 -002 & MOST 103-2811-M-492-004).

References

Central Weather Bureau of Taiwan (2011-2012) (Data for meteorological and seismic parameters). Retrieved from http://www.cwb.gov.tw

Chang LS, Chow M, Chen PY (1947) The Taiwan earthquake of December 5, 1946. Taiwan Geol Surv Bull 1:17–20

Choubey VM, Kumar N, Arora BR (2009) Precursory signatures in the radon and geohydrological borehole data for M4.9 Kharsali earthquake of Garhwal Himalaya. Sci Total Environ 407(22):5877–5883

Cicerone RD, Ebel JE, Britton J (2009) A systematic compilation of earthquake precursors. Tectonophysics 476:371–396

Einarsson P, Theodorsson P, Hjartardottir AR, Guojonsson GI (2008) Radon changes associated with the earthquake sequence in June 2000 in the South Iceland seismic zone. Pure Appl Geophys 165:63–74

Fraedrich K (1986) Estimating dimensions of weather and climate attractors. J Atmos Sci 43:419–432

Ghosh D, Deb A, Sengupta R (2009) Anomalous radon emission as precursor of earthquake. J Appl Geophys 69(2):67–81

Hartmann J, Levy KJ (2005) Hydrogeological and gasgeochemical earthquake precursors—a review for application. Nat Hazards 34:279–304

Hsu TL, Chang HC (1979) Quaternary faulting in Taiwan. Mem Geol Soc China 3:155–165

Hwang RD, Yu GK, Chang WY, Chang JP (2003) Lateral variations of shallow shear-velocity structure in Southwestern Taiwan inferred from short-period Rayleigh waves. Earth Planets Space 55:349–354

Italiano F, Martinelli G, Plescia P (2008) CO_2 degassing over seismic areas: the role of mechanochemical production at the study case of central apennines. Pure Appl Geophys 165:75–94

Kumar A, Singh S, Mahajan S, Bajwa BS, Kalia R, Dhar S (2009) Earthquake precursory studies in Kangra valley of North West Himalayas, India, with special emphasis on radon emission. Appl Radiat Isot 67:1904–1911

Kumar A, Walia V, Yang TF, Hsien C-H, Lin S-J, Eappen KP, Arora BR (2013a) Radon-thoron monitoring in Tatun volcanic areas of northern Taiwan using LR-115 alpha track detector technique: pre calibration and installation. Acta Geophys 61(4):958–976

Kumar G, Kumar A, Walia V, Kumar J, Gupta V, Yang TF, Singh S, Bajwa BS (2013b) Soil gas radon–thoron monitoring in Dharamshala area of North–West Himalayas, India using solid state nuclear track detectors. J Earth Syst Sci 122(5):1295–1301

Lee CT, Chen CT, Chi YM, Liao CW, Liao CF, Lin CC (2000) Engineering investigation of Hsinhua fault. Natl Cent Univ Report, 7 **(in Chinese)**

Ramola RC, Prasad Y, Prasad G, Kumar S, Choubey VM (2008) Soil-gas radon as seismotectonic indicator in Garhwal Himalaya. J Appl Radiat Isot 66:1523–1530

Stranden E, Kolstad AK, Lind B (1984) Radon exhalation: moisture and temperature dependence. Health Phys 47(3):480–484

Torkar D, Zmazek B, Vaupotič J, Kobal I (2010) Application of artificial neural networks in simulating radon levels in soil gas. Chem Geol 270(1–4):1–8

Ulomov VI, Mavashev BZ (1967) A precursor of a strong tectonic earthquake. Akad Sci USSR Earth Sci Sect 176:9–11

Vautard R, Ghil M (1989) Singular spectrum analysis in nonlinear dynamics, with applications to paleoclimatic time series. Phys D 35:395–424

Vautard R, Yiou P, Ghil M (1992) Singular-spectrum analysis: a toolkit for short, noisy chaotic signals. Phys D 58:95–126

Walia V, Su TC, Fu CC, Yang TF (2005) Spatial variations of radon and helium concentrations in soil-gas across the Shan-Chiao fault. North Taiwan Radiat Meas 40(2–6):513–516

Walia V, Yang TF, Lin S-J, Hong WL, Fu CC, Wen K-L, Chen C-H (2009) Continuous temporal soil-gas composition variations for earthquake precursory studies along Hsincheng and Hsinhua faults in Taiwan. Radiat Meas 44:934–939

Walia V, Yang TF, Lin S-J, Kumar A, Fu CC, Chiu J-M, Chang H-H, Wen K-L, Chen C-H (2013) Temporal variation of soil gas compositions for earthquake surveillance in Taiwan. Radiat Meas 50:154–159

Yang TF, Walia V, Chyi LL, Fu CC, Chen C-H, Liu TK, Song CS, Lee RY, Lee M (2005) Variations of soil radon and thoron concentrations in a fault zone and prospective earthquakes in SW Taiwan. Radiat Meas 40:496–502

Yang TF, Wen HY, Fu CC, Lee HF, Lan F, Chen AT, Hong L, Lin S-J, Walia V (2011) Soil radon flux and concentrations in hydrothermal area of the Tatun Volcano Group, Northern Taiwan. Geochem J 45:483–490

Zmazek B, Todorovski L, Džeroski S, Vaupotič J, Kobal I (2003) Application of decision trees to the analysis of soil radon data for earthquake prediction. Appl Radiat Isot 58(6):697–706